

Gas source molecular beam epitaxy of high quality $\text{Al}_x\text{Ga}_{1-x}\text{N}$ ($0 \leq x \leq 1$) on Si(111)

S. Nikishin,^{a)} G. Kipshidze, V. Kuryatkov, K. Choi, Iu. Gherasoiu, and L. Grave de Peralta

Department of Electrical Engineering, Texas Tech University, Lubbock, Texas 79401

A. Zubrilov and V. Tretyakov

Ioffe Physical-Technical Institute, 194021 St. Petersburg, Russia

K. Copeland, T. Prokofyeva, and M. Holtz

Department of Physics, Texas Tech University, Lubbock, Texas 79401

R. Asomoza and Yu. Kudryavtsev

SIMS Laboratory of SEES, Department of Electrical Engineering, CINVESTAV, Mexico D.F. 07300, Mexico

H. Temkin

Department of Electrical Engineering, Texas Tech University, Lubbock, Texas 79401

(Received 28 December 2000; accepted 9 April 2001)

Layers of $\text{Al}_x\text{Ga}_{1-x}\text{N}$, with $0 \leq x \leq 1$, were grown on Si(111) substrates by gas source molecular beam epitaxy with ammonia. We show that the initial formation of the Si–N–Al interlayer between the Si substrate and the AlN layer, at a growth temperature of 1130–1190 K, results in very rapid transition to two-dimensional growth mode of AlN. The transition is essential for subsequent growth of high quality GaN, $\text{Al}_x\text{Ga}_{1-x}\text{N}$, and AlGaN/GaN superlattices. The undoped GaN layers have a background electron concentration of $(2-3) \times 10^{16} \text{ cm}^{-3}$ and mobility up to $(800 \pm 100) \text{ cm}^2/\text{V s}$, for film thickness $\sim 2 \mu\text{m}$. The lowest electron concentration in $\text{Al}_x\text{Ga}_{1-x}\text{N}$, with $0.2 < x < 0.6$, was $\sim (2-3) \times 10^{16} \text{ cm}^{-3}$ for 0.5–0.7- μm -thick film. Cathodoluminescence and optical reflectance spectroscopy were used to study optical properties of these $\text{Al}_x\text{Ga}_{1-x}\text{N}$ layers. We found that the band gap dependence on composition can be described as $E_g(x) = 3.42 + 1.21x + 1.5x^2$. *p-n* junctions have been formed on crack-free layers of GaN with the use of Mg dopant. Light emitting diodes with peak emission wavelength at 3.23 eV have been demonstrated. © 2001 American Vacuum Society. [DOI: 10.1116/1.1377590]

I. INTRODUCTION

Structures based on GaN and $\text{Al}_x\text{Ga}_{1-x}\text{N}$, prepared on sapphire, are being developed for photodetectors¹⁻⁴ and light emitting diodes operating at wavelengths shorter than 360 nm. Many of these applications would benefit from $\text{Al}_x\text{Ga}_{1-x}\text{N}$ -based heterostructures grown on Si. Silicon is a very attractive substrate for the growth of GaN-related materials since large diameter wafers are available, having relatively high thermal conductivity and low cost. However, while some work has already been done to prepare $\text{Al}_x\text{Ga}_{1-x}\text{N}$ on Si(111) by molecular beam epitaxy (MBE),⁵⁻⁹ investigation of the crack formation process, dopant incorporation, and behavior of band gap versus composition in the range of Al content $x_{\text{AlN}} > 0.6$ are still not well understood.

Two growth nucleation methods are known to be effective for epitaxial nitride layers on Si substrates. The first method is carried out on the Si(111)- 7×7 reconstructed surface¹⁰⁻¹³ at a temperature below 830 °C. The procedure includes deposition of a few Al monolayers on the Si surface before the growth of AlN, to prevent the formation of the amorphous SiN_x . After that, the Al is nitrated and epitaxy of AlN is initiated. The second method, the formation of AlN at a

temperature higher than that of the $7 \times 7-1 \times 1$ surface reconstruction transition, relies on the formation of a Si–N–Al interlayer and the subsequent epitaxy of AlN.¹⁴

This work describes the preparation of AlGaN over the entire range of the AlN content. We also discuss the investigation of growth mechanisms leading to the suppression of cracks, effective dopant incorporation, and the preparation of light emitting diodes.

II. EXPERIMENTAL DETAILS

$\text{Al}_x\text{Ga}_{1-x}\text{N}$ films, with $0 \leq x \leq 1$, were grown by gas source molecular beam epitaxy (GSMBE) with ammonia on oriented *n*- and *p*-type Si(111) substrates. The substrates were prepared by wet chemical etching.¹⁴ The effects of growth conditions on the surface morphology, homogeneity of the film thickness, and the structure of epitaxial layers have been studied using 10 kV reflection high-energy electron diffraction (RHEED), low-energy electron diffraction (LEED), atomic force microscopy (AFM), x-ray diffraction, secondary ion mass spectroscopy, cathodoluminescence (CL), and optical reflectivity. Electrical parameters were investigated by capacitance–voltage (*C–V*), thermoprobe, and Hall measurements. Epitaxial layers grown on nitrated sapphire substrate¹⁵ were used for Hall measurements.

^{a)}Electronic mail: sergey.nikishin@coe.ttu.edu

Ammonia was introduced into the growth chamber through a mass-flow controller operating in the range of 50 sccm. The temperature was measured by a pyrometer, corrected for the emissivity of the substrate. The layers of AlN were grown in the temperature range of 860 ± 30 °C. Layers of GaN and AlGaIn were grown at 780 ± 20 °C.^{9,16} Si and Mg were used as dopants to obtain *n*- and *p*-type conductivities.

III. RESULTS AND DISCUSSION

Epitaxial growth of AlN is usually initiated with a few monolayers (2–3 ML) of Al.^{10–14} It is generally believed that this results in the formation of the Al–Si γ phase, thus preventing the formation of amorphous silicon nitride. Subsequent exposure to N would result in formation of the Si–Al–N interface, allowing for epitaxy of AlN. However, the details of this mechanism are not clear. Due to a large misfit between AlN and Si there is no possibility for formation of pseudomorphic AlN layer, even if all Al atoms are bonded to Si at the interface. Only islands of relaxed Si–Al–N can be formed by exposure to nitrogen.¹¹ These islands cannot produce complete coverage of the Si surface, resulting in openings in which active nitrogen can react with Si and form Si–N bonds.¹¹ This process would thus result in the presence of islands of AlN and Si–N at the surface of Si. Such a surface exposed to fluxes of Al and active nitrogen should produce domains of AlN with different surface polarities. This is similar to the growth of GaAs on Si(001), where both polarities of GaAs are produced.¹⁷ However, high quality films of AlN were obtained with this nucleation procedure when the growth was initiated at low temperature and continued at higher temperature under large III/V flux ratios.¹⁸ This suppresses either the Al- or N-terminated islands, depending on the choice of fluxes.

To improve the nucleation process we carried out growth experiments on Si(111) substrates, leading to complete surface coverage with the Si–N–Al interlayer. This was done by exposing the surface to alternating fluxes of Al and active N.

We began the growth process at high (>830 °C) temperature, where formation of the Al–Si γ phase is impossible due to the short lifetime of Al atoms on Si, by a brief exposure of the surface to NH_3 . At this point RHEED shows the presence of an ordered periodic structure on (111) silicon, which we attributed to strongly bound layer of chemisorbed N atoms (Fig. 1). RHEED shows that the surface layer is ordered and two dimensional. This observation is consistent with the superstructure reported on the surface of hexagonal silicon nitride.¹⁹

A typical RHEED pattern due to formation of ordered surface structure is shown in Fig. 1. Following Ref. 19, we suppose that this structure can be attributed to a 4×4 -reconstructed surface of SiN_x crystal at the growth temperature. This superstructure generates 8×8 reconstruction at room temperature. The inset of Fig. 1 displays the LEED pattern of the ordered SiN_x surface, which is in agreement with results of scanning tunneling microscopy and LEED investigation.¹⁹

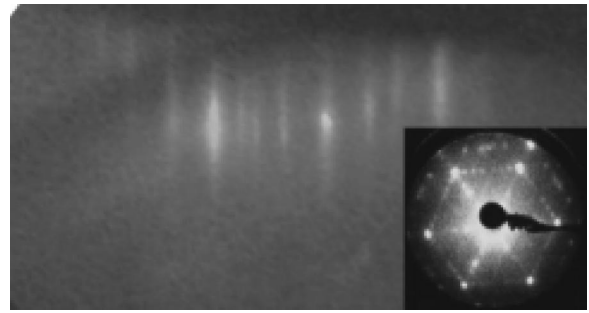


Fig. 1. RHEED picture of partially nitrated Si(111) surface at growth temperature and LEED pictures of partially nitrated Si(111) surface at room temperature.

Once the ordered structure of the type shown in Fig. 1 is formed, the surface is exposed to the flux of Al. This results in the formation of Si–N–Al islands, in agreement with previous observations, separated by the clean surface of Si. This surface is then exposed to active nitrogen, resulting in the formation of Si–N bonds over the clean Si surface. A second exposure to Al flux increases the surface coverage of Si–N–Al. This process of alternating exposure to Al and N is carried out several times, until a complete surface coverage with the Si–N–Al phase is obtained. At this point the growth surface is free of SiN_x .

By initiating the growth of AlN at a high temperature, it ensures that Al atoms form chemical bonds only with nitrogen atoms bonded to Si. Such a Si–N–Al interlayer would provide strongly oriented films with definite Al polarity. After formation of this layer is completed, growth of AlN can be started by simultaneous exposure to fluxes of Al and ammonia. The AlN and the subsequently grown GaN or AlGaIn show good crystalline properties, atomically smooth surfaces, and are free of cracks. Using this procedure we were able to grow AlGaIn over the entire range of composition, from GaN to AlN, on Si substrates.

It is well known that *p*-type conductivity in nitrides occurs when Mg is incorporated into Ga-substitutional sites.²⁰ It is also known that superior incorporation of Mg should take place on a metal-terminated surface.²¹ The stoichiometry of the growth surface is thus important. We optimize the NH_3/Ga flux ratio and the substrate temperature for the doping process, with the goals of reaching the two-dimensional growth mode and creation of the desired Ga-substitutional sites on the growing surface. The parameter window that yields the stoichiometric surface with a two-dimensional periodicity, corresponding to a bilayer structure, is quite narrow and different for different growth rates. Figure 2 shows the typical evolution of GaN and AlGaIn growth rates versus NH_3 flux. The growth rate progresses until the V/III ratio is saturated for constant volume of the incident flux of group III materials. The turning points demonstrate V/III ratio close to unity and the boundary between Ga-rich and N-rich conditions. This growth optimization was carried out at the substrate temperature below 800 °C. The optimization of the V/III ratio during the growth of AlGaIn shows unexpected behavior. In this experiment, sources of Ga and Al were kept

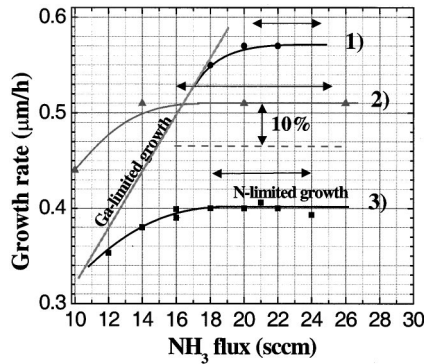


FIG. 2. Growth rate of GaN and $\text{Al}_x\text{Ga}_{1-x}\text{N}$ vs NH_3/Ga flux ratio.

at a constant temperature. By measuring growth rates of GaN and AlN as a function of ammonia flux, the expected AlGaIn growth rate could be estimated (shown by a dashed line) and compared to the experimental value. The growth rate of AlGaIn is higher, under N-rich conditions, than the expected growth rate.

The difference between the measured and calculated growth rates is about 10%. This can be explained by the enhanced cracking efficiency of ammonia in the presence of Al. The possible influence of increased cracking efficiency on the quality of AlGaIn, and its role in the doping efficiency, is still under study, but it is clear that this effect makes *p*-type doping AlGaIn more difficult.

The results of band gap measurements of AlGaIn by optical reflectance are illustrated in Fig. 3. In addition, Fig. 3 also shows absorption data obtained on AlGaIn samples grown by MBE on sapphire²² and CL data obtained on our layers grown on Si.⁹ The three sets of data show the same band gap dependence on composition, described by $E_g(x) = 3.42 + 1.21x + 1.5x^2$. The bowing coefficient $b = 1.5$ eV is close to that determined previously for AlGaIn prepared on different substrates, by a variety of growth methods.^{9,22–24} This value of b is larger than that predicted from the lattice constant difference between GaN and AlN, and may be due

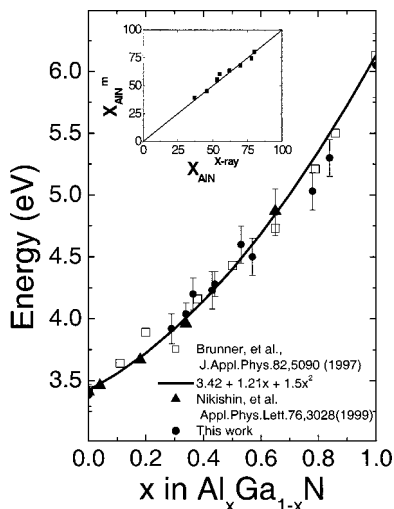
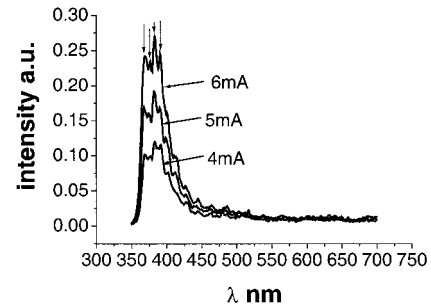


FIG. 3. Band gap dependence of $\text{Al}_x\text{Ga}_{1-x}\text{N}$ layers vs the composition.

p-GaN:Mg
$d=0.4\mu\text{m}$
(<i>p</i> -type by thermoprobe measurements)
Undoped GaN $\approx 40\text{--}60\text{ nm}$
n-GaN:Si ($n > 10^{18}\text{ cm}^{-3}$);
$d=1.8\mu\text{m}$
AlGaIn/GaN
Short period SL
GaN $d=0.15\mu\text{m}$
AlGaIn/GaN
Short period SL
AlN $\approx 40\text{ nm}$
n-Si

a)



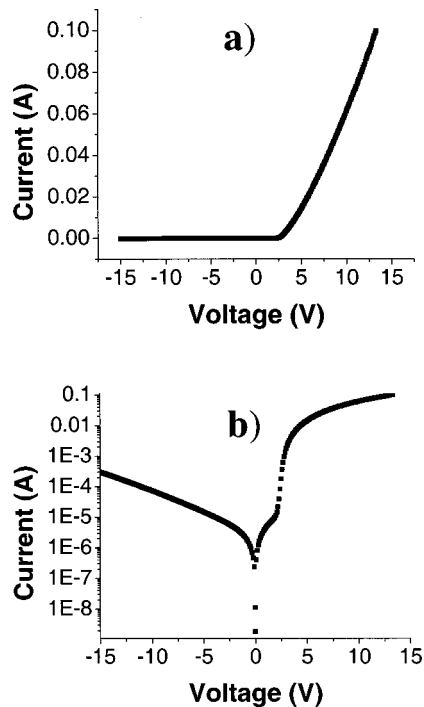
b)

FIG. 4. Cross section (a) and electroluminescence spectra (b) of GaN LED.

to a large scattering potential for electrons in this alloy system.²⁴ The inset of Fig. 3 shows the relationship between lattice constant measurements, by x-ray diffraction and x-ray fluorescence measurements. Agreement between the methods is clear. The CL peak wavelength of the bandedge emission varied from 3.406 eV (364.0 nm) for GaN to 4.98 eV (249.0 nm) for $\text{Al}_{0.8}\text{Ga}_{0.2}\text{N}$. Agreement between optical reflectance and CL measurements was also observed. This result is consistent with the low carrier concentration of our layers. Hall and *C-V* measurements show electron concentrations in the alloy in the range of $(10^{16}\text{--}10^{17})\text{ cm}^{-3}$. The lowest electron concentration in $\text{Al}_x\text{Ga}_{1-x}\text{N}$, with $0.2 < x < 0.6$, was about $(2\text{--}3) \times 10^{16}\text{ cm}^{-3}$. The best undoped GaN samples show residual electron concentrations of $(2\text{--}3) \times 10^{16}\text{ cm}^{-3}$ and Hall mobilities of $800 \pm 100\text{ cm}^2/\text{V s}$, at room temperature.

The arrows in Fig. 2 show growth conditions for GaN and AlGaIn corresponding to the maximum Mg incorporation rate of $\sim 3 \times 10^{20}\text{ cm}^{-3}$. At these conditions we measured hole concentration $p = (0.7\text{--}1) \times 10^{18}\text{ cm}^{-3}$ and mobility $\mu_p = 50 \pm 10\text{ cm}^2/\text{V s}$ at room temperature. Maximum hole concentration, which was achieved under Ga deficient conditions, is $2 \times 10^{18}\text{ cm}^{-3}$ for GaN:Mg and $5 \times 10^{16}\text{ cm}^{-3}$ for $\text{Al}_{0.05}\text{Ga}_{0.95}\text{N:Mg}$. All Mg-doped samples showed *p*-type conductivity as grown. No improvement in Mg activation was observed in postgrowth annealing experiments. Moreover, such annealing changed the conductivity type from *p* to *n*, in agreement with Ref. 25. Details of Mg and H distribution in GaN and AlGaIn layers are discussed elsewhere.²⁶

Light emitting diode (LED) structures with total thicknesses $\sim 2.5\mu\text{m}$ were grown in the two-dimensional growth

FIG. 5. I - V of GaN LED.

mode at ~ 800 °C and GaN growth rate of ~ 0.7 $\mu\text{m}/\text{h}$. No crack formation was observed. Root-mean-square surface roughness measured by AFM was ~ 0.7 nm for areas 20 $\mu\text{m} \times 20$ μm . A cross-section of the LED structure consisting 40 nm AlN layer/buffer superlattice of undoped (AlGaIn/GaN)/undoped 0.15 μm GaN spacer/buffer superlattice of undoped (AlGaIn/GaN)/1.8 μm of Si-doped GaN/10 nm of undoped GaN/0.5 μm of Mg doped GaN is shown in Fig. 4(a). p -type contacts were made with InZn alloy annealed at 400 °C for 2–5 min. Large area gold contact was used at the backside of low-resistivity n -Si substrate. The room temperature electroluminescence spectra are shown as a function of current in Fig. 4(b). The emission was dominated by a peak at ~ 380 nm ($h\nu_{\text{max}} \sim 3.23$ eV). This value is close to that observed from LEDs grown by plasma-assisted MBE²⁷ and GSMBE with ammonia on sapphire.²⁸ We believe that slightly long wavelength emission peak position of our LED compared with single, $\lambda \sim 365$ nm,⁷ and double, $\lambda \sim 360$ nm⁵ GaN/AlGaIn LED heterostructures grown on Si substrates can be attributed to radiative recombination in the undoped n -GaIn and Mg-doped p -GaIn layers close to the p - n junction area. We estimate the hole concentration in the p -GaIn layer at $\sim (3-5) \times 10^{17}$ cm^{-3} . The spectra show Fabry-Perot interference fringes, consistent with flat epitaxial interfaces.²⁸

A typical room temperature current-voltage (I - V) curve from a vertical geometry LED is shown in Fig. 5. Under forward bias, diodes start to emit at ~ 3.6 eV. At reverse bias, leakage currents at -10 V were in the 10–100 μA range, for different diodes.

In summary, we describe growth procedures resulting in high quality AlGaIn on Si substrates. Gas source MBE growth under stoichiometric conditions allowed us to control electrical properties of layers and structures. Light emitting diodes based on GaN grown on Si operate at low currents and forward voltage.

ACKNOWLEDGMENTS

Work at Texas Tech University was supported by DARPA, NSF, J. F. Maddox Foundation, and SBCCOM. Work at CINVESTAV was supported by Conacyt, Mexico (Grant No. 31106-U).

- ¹B. W. Lim, Q. C. Chen, J. Y. Yang, and M. A. Khan, *Appl. Phys. Lett.* **68**, 3761 (1996).
- ²A. Osinsky, S. Gangopadhyay, B. W. Lim, M. Z. Anwar, M. A. Khan, D. Kuksenkov, and H. Temkin, *Appl. Phys. Lett.* **72**, 742 (1998).
- ³G. Parish *et al.*, *Appl. Phys. Lett.* **75**, 247 (1999).
- ⁴F. Omnès, N. Marengo, B. Beaumont, Ph. de Mierry, E. Monroy, F. Calle, and E. Muñoz, *J. Appl. Phys.* **86**, 5286 (1999), and references therein.
- ⁵S. Guha and N. A. Bojarzuk, *Appl. Phys. Lett.* **72**, 415 (1998).
- ⁶S. Guha and N. A. Bojarzuk, *Appl. Phys. Lett.* **72**, 1487 (1998).
- ⁷M. A. Sánchez-García, F. B. Narajo, J. L. Pau, A. Jimenez, E. Calleja, and E. Muñoz, *J. Appl. Phys.* **87**, 1569 (2000).
- ⁸J. L. Pau, E. Monroy, F. B. Narajo, E. Muñoz, F. Calle, M. A. Sánchez-García, and E. Calleja, *Appl. Phys. Lett.* **76**, 2785 (2000).
- ⁹S. A. Nikishin, N. N. Faleev, A. S. Zubrilov, V. G. Antipov, and H. Temkin, *Appl. Phys. Lett.* **76**, 3028 (2000).
- ¹⁰E. Calleja, M. A. Sánchez-García, E. Monroy, F. J. Sánchez, E. Muñoz, A. Sanz-Hervás, C. Villar, and M. Aguilar, *J. Appl. Phys.* **82**, 4681 (1997).
- ¹¹K. Yasutake, A. Takeuchi, H. Kakiuchi, and K. Yoshii, *J. Vac. Sci. Technol. A* **16**, 2140 (1998).
- ¹²E. S. Hellman, D. N. E. Buchanan, and C. H. Chen, *MRS Internet J. Nitride Semicond. Res.* **3**, 43 (1998).
- ¹³G. Kipshidze *et al.*, *Semiconductors* **33**, 1241 (1999), and references therein.
- ¹⁴S. A. Nikishin *et al.*, *Appl. Phys. Lett.* **75**, 484 (1999).
- ¹⁵N. Grandjean, J. Massies, and M. Leroux, *Appl. Phys. Lett.* **69**, 2071 (1996).
- ¹⁶S. A. Nikishin *et al.*, *Appl. Phys. Lett.* **75**, 2073 (1999).
- ¹⁷See, for example, V. G. Antipov *et al.*, *Sov. Tech. Phys. Lett.* **18**, 26 (1992), and references therein.
- ¹⁸G. Kipshidze, Wo. Richter, and H. Schenk, *detsches patent—Und Markenamt*, DE19827198A1 (June 18, 1998).
- ¹⁹X. Wang, G. Zhai, J. Yang, and N. Cue, *Phys. Rev. B* **60**, R2146 (1999), and references therein.
- ²⁰C. G. Van de Walle, C. Stampfl, and J. Neugebauer, *J. Cryst. Growth* **189/190**, 505 (1998).
- ²¹T. S. Cheng, S. V. Novikov, C. T. Foxon, and J. W. Orton, *J. Cryst. Growth* **109**, 439 (1999).
- ²²D. Brunner, H. Angerer, E. Bustarret, F. Freudenberg, R. Höppler, R. Dimitrov, O. Ambacher, and M. Stutzmann, *J. Appl. Phys.* **82**, 5090 (1997).
- ²³M. R. H. Khan, Y. Koide, H. Itoh, N. Sawaki, and I. Akasaki, *Solid State Commun.* **50**, 509 (1986).
- ²⁴A. S. Zubrilov, Yu. V. Melnik, A. E. Nikolaev, D. V. Tsvetkov, V. V. Tretyakov, M. A. Jakobson, D. K. Nelson, and V. A. Dmitriev, *2nd Russian Workshop Gallium Nitride, Indium Nitride, Aluminum Nitride: Structure and Devices*, 2 June 1998, St. Petersburg, Russia, p. 34 (in Russian).
- ²⁵W. Kim, A. E. Botchkarev, A. Salvador, G. Popovici, H. Tang, and H. Morkoç, *J. Appl. Phys.* **82**, 219 (1997).
- ²⁶S. Nikishin, G. Kipshidze, K. Kuryatkov, Yu. Kudryavtsev, R. Asomoza, and H. Temkin (unpublished).
- ²⁷R. P. Vaudo, I. D. Goepfert, T. D. Moustakas, D. M. Beyea, T. J. Frey, and K. Meehan, *J. Appl. Phys.* **79**, 2779 (1996).
- ²⁸N. Grandjean, J. Massies, M. Leroux, and P. Lorenzini, *Appl. Phys. Lett.* **72**, 82 (1998).